AVNA - Based Polarimetric Scatterometers

Fawwaz T. Ulaby
Michael W. Whitt, and
Kamal Sarabandi
Radiation Laboratory
Dept. of Electrical Engineering and Computer Science
University of Michigan
Ann Arbor, Michigan

Abstract

A polarimetric radar is an instrument capable of measuring the radar cross section (RCS), of a target of interest, for any desired combination of transmit and receive antenna polarizations. The polarimetric capability can be realized by a hardware implementation, which requires relatively complicated RF circuitry, or by a polarization-synthesis software implementation, with much simpler RF requirements. The polarization-synthesis technique is equally applicable to both imaging systems, such as the synthetic aperture radar (SAR), and to non-imaging scatterometers, used to characterize the scattering properties of point and distributed targets. With the recent introduction of the Automatic Vector Network Analyzer (AVNA), making accurate measurements of both the magnitude and phase of the scattered signal is now possible by using the signal-processing and error-correction techniques of the network analyzer. Because this new approach is rapidly becoming the standard technique for measuring the polarimetric response of point and distributed targets, this paper[1] was prepared to provide an overview of AVNA-based scatterometer configurations in use today at centimeter and millimeter wavelengths.

1. Polarization Synthesis for a Point Target

1.1 Wave Polarization

When considering problems involving scattering from the earth's surface, we often conveniently represent the earth's surface by the *x-y* plane, and represent the polarization vector of waves incident upon or scattered from the surface in terms of the spherical angles, θ and ϕ. For a plane wave traveling in the direction $\hat{\mathbf{k}}$, as shown in Figure 1, we customarily characterize the electric field vector, $\mathbf{E}$, in terms of a *horizontal polarization* component, $E_h\hat{\mathbf{h}}$, and a *vertical polarization* component, $E_v\hat{\mathbf{v}}$, defined such that the coordinate system $(\hat{\mathbf{k}},\hat{\mathbf{v}},\hat{\mathbf{h}})$ coincides with $(\hat{\mathbf{r}},\hat{\theta},\hat{\phi})$ of a standard spherical coordinate system. Thus,

$$\mathbf{E} = (E_v\hat{\mathbf{v}} + E_h\hat{\mathbf{h}})e^{ik\hat{\mathbf{k}}\cdot\mathbf{r}} \tag{1}$$

[1]Some of the material in this paper also appeared in the recently-published book, *Radar Polarimetry for Geoscience Applications*, edited by Ulaby and Elachi, Artech House, 1990.

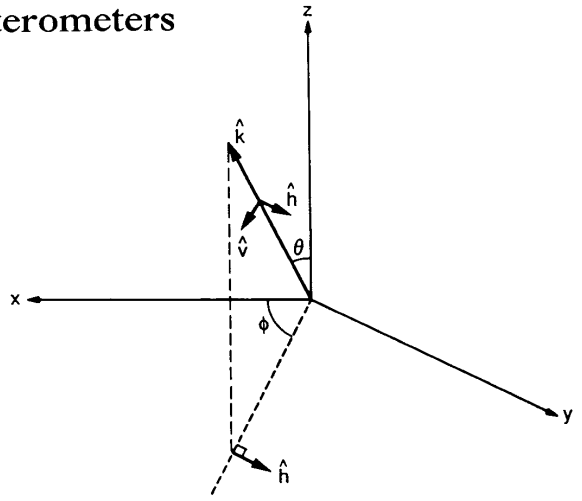

Figure 1. Plane wave propagating in direction $\hat{\mathbf{k}}$, with E-vector components E_v and E_h defined such that $\hat{\mathbf{h}}=(\hat{\mathbf{k}}\times\hat{\mathbf{z}})/|\hat{\mathbf{k}}\times\hat{\mathbf{z}}|$ and $\hat{\mathbf{v}}=\hat{\mathbf{h}}\times\hat{\mathbf{k}}$.

with

$$\hat{\mathbf{h}} = \frac{\hat{\mathbf{z}}\times\hat{\mathbf{k}}}{|\hat{\mathbf{z}}\times\hat{\mathbf{k}}|} = -\sin\phi\hat{\mathbf{x}} + \cos\phi\hat{\mathbf{y}} \tag{2}$$

$$\hat{\mathbf{v}} = \hat{\mathbf{h}}\times\hat{\mathbf{k}} = \cos\theta\cos\phi\hat{\mathbf{x}} + \cos\theta\sin\phi\hat{\mathbf{y}} - \sin\theta\hat{\mathbf{z}}, \tag{3}$$

and

$$\hat{\mathbf{k}} = \sin\theta\cos\phi\hat{\mathbf{x}} + \sin\theta\sin\phi\hat{\mathbf{y}} + \cos\theta\hat{\mathbf{z}}, \tag{4}$$

where $k = 2\pi/\lambda$ is the wave number. As will prove useful in later sections, we shall adopt the matrix notation

$$\mathbf{E} = \begin{bmatrix} E_v \\ E_h \end{bmatrix} \tag{5}$$

wherein the phase factor of (1) has been suppressed for convenience.

The amplitudes E_v and E_h are, in general, complex quantities given by

$$E_v = a_v e^{-i\delta_v} \tag{6}$$

$$E_h = a_h e^{-i\delta_h} \tag{7}$$

where a_v and a_h are the magnitudes of E_v and E_h, respectively, and δ_v and δ_h are their phase angles. The

polarization of the wave, which describes the shape and locus of the tip of the *E*-vector (in a plane orthogonal to the direction of propagation) as a function of time, is specified by the parameters α and δ given by the relations

$$\tan \alpha = \frac{a_h}{a_v} \tag{8}$$

$$\delta = \delta_h - \delta_v. \tag{9}$$

In the general case, the locus of the *E*-vector is an ellipse (Figure 2), and the wave is called elliptically polarized. For certain values of α and δ, the ellipse may degenerate into a straight line ($\delta=0$) or a circle ($\alpha=\pi/4$ and $\delta=\pm\pi/2$), in which case the polarization is called *linear* or *circular*, respectively. The *sense of rotation* of the *E*-vector in the plane of polarization is called the *sense of polarization*, or *handedness*. The sense is called *right-handed* (*left-handed*) if the direction of rotation (in a plane at a fixed r) is *clockwise* (*counterclockwise*) for an observer looking in the direction of propagation [2, p. 76].

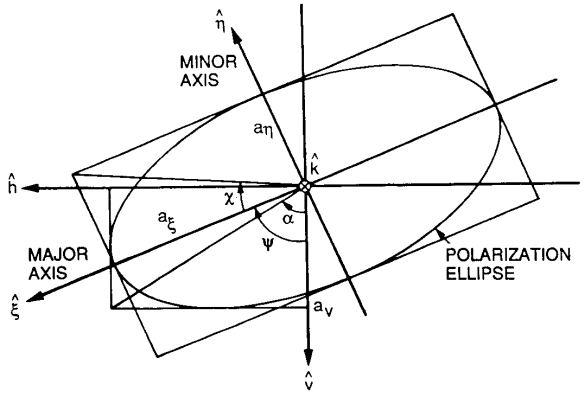

Fig. 2. Polarization ellipse in the *v-h* plane for a wave traveling in the $\hat{k}$ direction.

The polarization ellipse (Figure 2) is characterized by the *rotation angle* ψ and *ellipticity angle* χ, which are related to α and δ by

$$\tan 2\psi = (\tan 2\alpha) \cos \delta \tag{10}$$

$$\sin 2\chi = (\sin 2\alpha) \sin \delta \tag{11}$$

and, conversely,

$$\cos 2\alpha = (\cos 2\chi)(\cos 2\psi) \tag{12}$$

$$\tan \delta = \sec 2\chi \ . \tag{13}$$

1.2 Scattering Matrix

Consider a scattering object, located at the center of the coordinate system shown in Figure 3, illuminated by a plane wave radiated by a transmitting antenna in the direction $\hat{\mathbf{k}}_t$, and composed of vertical

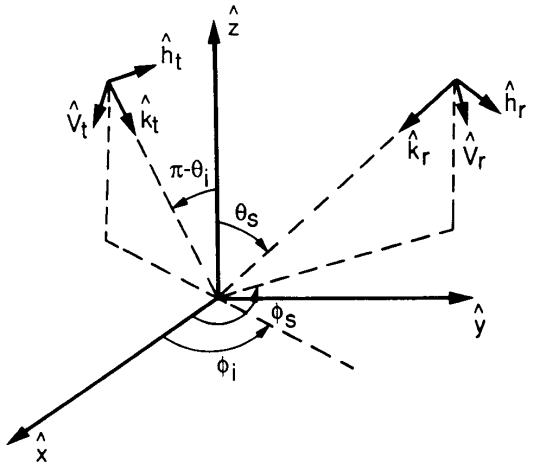

Fig. 3. Coordinate systems and scattering geometry for the backscatter alignment (BSA) convention.

and horizontal polarization components $\hat{\mathbf{v}}_t$ and $\hat{\mathbf{h}}_t$, respectively. Scattering calculations usually are performed using either the forward scattering alignment (FSA) convention, for which the polarization unit vectors of the scattered wave are defined with respect to the direction of propagation of the scattered wave, or according to the backscatter alignment (BSA) convention shown in Figure 3, for which the polarization unit vectors are defined with respect to the radar antenna in accordance with the IEEE standard [2, p. 76]. According to the BSA convention, which we shall use exclusively in this paper, the polarization state of an antenna is defined to be the polarization of the wave radiated by the antenna, even when it is used as a receiving antenna.

In the BSA convention, the transmitted and received fields are given by

$$\mathbf{E}^t = E_v^t \hat{\mathbf{v}}_t + E_h^t \hat{\mathbf{h}}_t, \tag{14}$$

$$\mathbf{E}^r = E_v^r \hat{\mathbf{v}}_r + E_h^r \hat{\mathbf{h}}_r, \tag{15}$$

and are related to each other by [3, 4]:

$$\mathbf{E}^r = \frac{e^{ikr}}{r} \mathbf{S}\, \mathbf{E}^t \tag{16}$$

where r is the distance between the scatterer and the receiving antenna and $\mathbf{S}$ is the *scattering matrix* of the scattering object, defined by

$$\mathbf{S} = \begin{bmatrix} S_{vv} & S_{vh} \\ S_{hv} & S_{hh} \end{bmatrix}. \tag{17}$$

In the general bistatic case, the scattering ampli-

tudes, S_{ij}, with $i,j = v$ or h, are each a function of both the incident and scattered angles, (θ_i,ϕ_i) and (θ_S,ϕ_S). For the monostatic radar case, wherein the transmit and receive antennas are co-located or the same antenna is used for both functions, the angles are related by $\theta_s = \pi-\theta_i$ and $\phi_i = \pi+\phi_i$, and the transmit and receive unit vectors become coincident: $(\hat{\mathbf{k}}_t, \hat{\mathbf{h}}_t, \hat{\mathbf{v}}_t) = (\hat{\mathbf{k}}_r, \hat{\mathbf{h}}_r, \hat{\mathbf{v}}_r)$.

1.3 Polarization Synthesis

The function of a polarimetric scatterometer is to measure the scattering matrix, **S**, by applying equation (16). The factor e^{ikr}/r can be determined by measuring the field backscattered from a target with a known scattering matrix, such as a metallic sphere. Upon transmitting a vertically polarized wave, $\mathbf{E}^t=E^t_v\hat{\mathbf{v}}_t$, and recording both components of the received wave using a dual-polarized antenna, we can determine the scattering amplitudes S_{vv} and S_{hv} from

$$S_{vv} = \left[\frac{e^{ikr}}{r}\right]^{-1} \cdot \frac{E^r_v}{E^t_v} \tag{18}$$

$$S_{hv} = \left[\frac{e^{ikr}}{r}\right]^{-1} \cdot \frac{E^r_h}{E^t_v} \tag{19}$$

A similar procedure involving the transmission of a horizontally polarized wave leads to the determination of S_{vh} and S_{hh}. The scattering amplitudes are complex quantities, which means that the scatterometer has to be able to measure both the magnitudes and phases of the received-field components relative to those of the transmitted field. In practice, however, it is not necessary to know the magnitudes and associated phases of all four scattering amplitudes in order to perform polarization synthesis; it is sufficient to know the four magnitudes and the phases of any three of the scattering amplitudes relative to the phase of the fourth. Furthermore, for the backscattering case (which is the only situation we are considering in this paper), we can invoke the reciprocity relation

$$S_{hv} = S_{vh} \tag{20}$$

to further reduce the number of quantities needed to characterize **S** down to five.

With **S** known, the radar cross section (RCS) for any of the principal linear polarization combinations can be obtained from

$$\sigma_{ij} = 4\pi|S_{ij}|^2; \quad i,j = v \text{ or } h\ . \tag{21}$$

For any other combination of transmit and receive polarizations, defined by the polarization angles (ψ_t,χ_t) and (ψ_r,χ_r), the radar cross section can be computed by applying the *polarization-synthesis equation* [4]

$$\sigma(\psi_r,\chi_r;\psi_t,\chi_t) = 4\pi|\mathbf{p}^r\bullet\mathbf{S}\mathbf{p}^t|^2\ , \tag{22}$$

where $\mathbf{p}^r$ and $\mathbf{p}^t$ are the polarization vectors of the receive and transmit antennas,

$$\mathbf{p}^m = \frac{\mathbf{E}^m}{|\mathbf{E}^m|} = \begin{bmatrix} \cos\alpha_m \\ \sin\alpha_m\, e^{-i\delta_m} \end{bmatrix}, \quad m = r \text{ or } t, \tag{23}$$

with (α_m,δ_m) being related to (ψ_m,χ_m) by (12) and (13). Thus, knowledge of the matrix **S** permits calculation of the RCS of the object for any possible combination of elliptical transmit and receive antenna polarizations, including linear and circular polarizations.

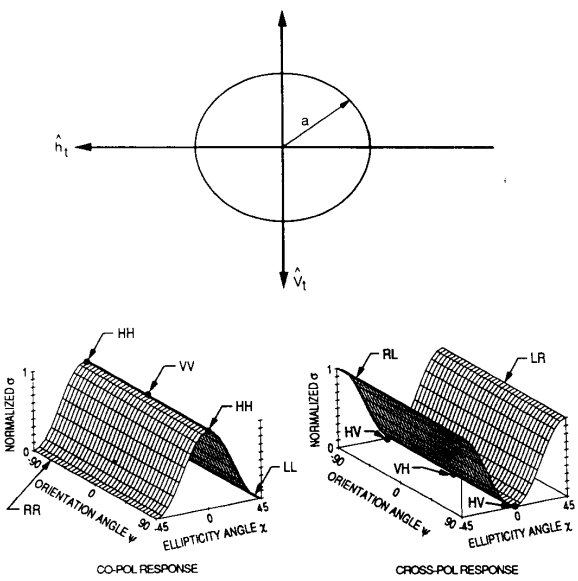

Fig. 4. Polarization responses of a large conducting sphere.

The *polarization response* provides a convenient graphical representation of the variation of the scattering cross section, σ, as a function of polarization. An example is shown in Figure 4 for a large metal sphere. It consists of two plots displaying σ as a function of ψ_t and χ_t, with one of the plots representing the co-polarized response, $\sigma(\psi_r=\psi_t,\ \chi_r=\chi_t)$, and the other representing the cross-polarized response, $\sigma(\psi_r=\psi_t+\pi/2,\ \chi_r=-\chi_t)$. For convenience, the plots are normalized such that the peak value is 1.0.

2. Polarization Synthesis for a Distributed Target

Unlike point targets, soil surfaces and vegetation canopies are distributed targets, composed of randomly-distributed scatterers. The backscattering behavior of a distributed target is characterized by the backscattering coefficient, σ^0, which is the ensemble average of the radar cross section, σ, per unit area,

$$\sigma^0 = \frac{<\sigma>}{A}\ , \tag{24}$$

where A is the illuminated area. For the principal linear polarizations, the synthesis process is straightforward: simply measure $\mathbf{S}$ for each of many independent samples of the distributed target (or pixels of resolution area A, in the case of an imaging radar), and then compute

$$\sigma^0_{ij} = \frac{4\pi}{AN} \sum_{l=1}^{N} |S_{ij}|^2_l, \; i,j = v \text{ or } h, \tag{25}$$

where N is the number of independent samples measured. For other polarization combinations of transmit and receive polarizations, two approaches are available, both of which provide identical results.

2.1 Scattering Matrix Approach

The first approach is basically identical to the synthesis technique used in conjunction with point targets. Thus,

$$\sigma^0(\psi_r,\chi_r;\psi_t,\chi_t) = \frac{4\pi}{AN} \sum_{l=1}^{N} |\mathbf{p}^r \bullet \mathbf{S}_l \mathbf{p}^t|^2 \tag{26}$$

where $\mathbf{S}_l$ is the measured scattering matrix of the lth sample

2.2 Stokes Scattering Operator Approach

Instead of synthesizing the backscatter N times and then averaging the sum to obtain σ^0, as outlined in the proceeding approach, it is possible to use a computationally more efficient approach, based on the *Stokes scattering operator* [1, p. 32]. To show the procedure, we start with the *modified Stokes vector* representation of a polarized wave:

$$\mathbf{F}_m(\psi,\chi) = \begin{bmatrix} |E_v|^2 \\ |E_h|^2 \\ 2\mathrm{Re}(E_v E_h^*) \\ 2\mathrm{Im}(E_v E_h^*) \end{bmatrix} = \begin{bmatrix} a_v^2 \\ a_h^2 \\ 2a_v a_h \cos\delta \\ 2a_v a_h \sin\delta \end{bmatrix}$$

$$= \begin{bmatrix} \frac{1}{2}(1+\cos 2\psi \cos 2\chi) \\ \frac{1}{2}(1-\cos 2\psi \cos 2\chi) \\ \sin 2\psi \cos 2\chi \\ \sin 2\chi \end{bmatrix} I_0 \tag{27}$$

where $I_0 = a_v^2 + a_h^2$, and all other quantities were defined earlier, in Section 1. Upon applying (16), it can be shown [5, 6] that the transmitted and scattered modified Stokes vectors are related by the *modified Mueller Matrix* $\mathscr{L}_m$,

$$\mathbf{F}^r_m = \frac{1}{r^2} \mathscr{L}_m \mathbf{F}^t_m, \tag{28}$$

with the elements of $\mathscr{L}_m$ being real quantities, given in terms of the elements of the scattering matrix $\mathbf{S}$.

$$\mathscr{L}_m = \begin{bmatrix} |S_{vv}|^2 & |S_{vh}|^2 & \\ |S_{hv}|^2 & |S_{hh}|^2 & \\ 2\mathrm{Re}(S_{vv}S_{hv}^*) & 2\mathrm{Re}(S_{vh}S_{hh}^*) & \cdots \\ 2\mathrm{Im}(S_{vv}S_{hv}^*) & 2\mathrm{Im}(S_{vh}S_{hh}^*) & \end{bmatrix}$$

$$\cdots \begin{bmatrix} \mathrm{Re}(S_{vh}^* S_{vv}^*) & -\mathrm{Im}(S_{vh}^* S_{vv}^*) \\ \mathrm{Re}(S_{hh}^* S_{hv}^*) & -\mathrm{Im}(S_{hv}^* S_{hh}^*) \\ \mathrm{Re}(S_{vv}S_{hh}^* + S_{vh}S_{hv}^*) & -\mathrm{Im}(S_{vv}S_{hh}^* - S_{vh}S_{hv}^*) \\ \mathrm{Im}(S_{vv}S_{hh}^* + S_{vh}S_{hv}^*) & \mathrm{Re}(S_{vv}S_{hh}^* - S_{vh}S_{hv}^*) \end{bmatrix} \tag{29}$$

For a point target, the following polarization synthesis equation is applicable [4, 7]:

$$\sigma(\psi_r,\chi_r;\psi_t,\chi_t) = 4\pi \mathbf{A}^r_m \bullet \mathbf{M}_m \mathbf{A}^t_m \tag{30}$$

where $\mathbf{A}^r_m$ and $\mathbf{A}^t_m$ are the normalized modified Stokes vectors for the receive and transmit antennas ($\mathbf{A}_m = \mathbf{F}_m / I_0$), and $\mathbf{M}_m$ is known as the *Stokes scattering operator*, and is related to $\mathscr{L}_m$ by

$$\mathbf{M}_m = \mathbf{Q}\, \mathscr{L}_m, \tag{31}$$

with $\mathbf{Q}$ being a diagonal transformation matrix given by

$$\mathbf{Q} = \begin{bmatrix} 1 & 0 & 0 & 0 \\ 0 & 1 & 0 & 0 \\ 0 & 0 & 1/2 & 0 \\ 0 & 0 & 0 & -1/2 \end{bmatrix} \tag{32}$$

In the case of a distributed target for which N measurements of $\mathbf{M}_m$ are available, the backscattering coefficient can be synthesized for any transmit and receive antenna polarizations from

$$\sigma^0(\psi_r,\chi_r;\psi_t,\chi_t) = \frac{4\pi}{A} \mathbf{A}^r \bullet <\mathbf{M}_m> \mathbf{A}^t \tag{33}$$

where

$$<\mathbf{M}_m> = \frac{1}{N} \sum_{l=1}^{N} (\mathbf{M}_m)_l. \tag{34}$$

Because the averaging over the index l is performed prior to applying the synthesis equation (33), this approach has been found to be computationally superior to the direct synthesis approach presented in Section 2.1 [1, p.32]. Furthermore, this approach allows the use of a measurement process that circumvents a phase-stability problem associated with conducting polarimetric radar measurements under field conditions. More details on this problem are provided in Section 6.

3. AVNA - Based Polarimetric Scatterometers

Techniques available for measuring the polarimetric scattering response of targets are of three types: (1) fully coherent; (2) coherent-on-receive; and (3) incoherent. The incoherent technique is the standard approach used at optical wavelengths, because it is difficult to directly measure the phase difference between the *h*- and *v*-polarized components of the received signal. The technique is fairly laborious, and requires measurement of the received intensity with various combinations of polarizers placed in the path of the transmitted beam, and in front of the detector.

The fully-coherent technique is the simplest to implement using the *Automatic Vector Network Analyzer (AVNA)*, but it has strict requirements on phase stability over the time period it takes to complete the measurements of the four elements of the scattering matrix, S. Phase stability includes phase stability of the instrument, as well as the "phase" of the target. In a laboratory setting, the target is stationary, but when measuring distributed targets under natural conditions, such as a vegetation canopy, wind-caused movements of the scattering elements (leaves, etc.) change the scattering behavior of the target, particularly the phase part. The change in target phase is related to variations in the spatial positions of the scattering elements relative to the radar antenna. Whereas such variations are of minor consequence at the longer wavelengths in the microwave region, they can cause large errors in the measurement of S at millimeter wavelengths, particularly when the variations occur over time scales shorter than the time available to complete an individual measurement of the matrix, S. With a network analyzer-based scatterometer, the measurement time is typically 0.1-1 s.

The coherent-on-receive technique provides a solution for the phase-stability problem, as discussed later, in Section 6. Because it is a specialized technique, however, we will ignore it for the time being, and we will focus our attention exclusively on the more generic, fully-coherent approach, both in the remainder of this section and in the next two sections.

4. Network Analyzer Principles of Operation

In recent years, vector network analyzers have become widely available through a number of companies (Hewlett Packard, Wiltron, and other manufacturers), and they have been used as the basic component for polarimetric scatterometer systems [8-11].

In general, network analyzers measure the magnitude and phase characteristics of linear networks relative to some standard or reference. This is accomplished by making both transmission and reflection measurements, to obtain specific characteristics of the network (see Figure 5). For transmission measurements, the signal transmitted through the test network is compared to the incident signal, which serves as the reference. For reflection measurements, the signal reflected from the input port is compared with the incident signal. The output port, in this case, is usually terminated with a matched load, to remove reflections that travel back through the network and contribute to the reflected signal.

A basic vector network analyzer system consists of (1) an RF source, (2) an RF-to-IF converter, (3) an IF signal detector and analog-to-digital (A/D) converter, and (4) a digital microprocessor and display. In the context of Figure 5, the RF source is used to supply the incident signal to the test network. The transmitted or reflected RF signal, and a sample of the incident signal, are then mixed down to the IF range, maintaining the magnitude and phase relationships between the two signals. The IF signals are then detected, converted to digital form, and processed to obtain information about the test network. If a frequency-swept incident signal is used, the result is a measurement of the frequency response of the network, and Fourier transform techniques can be used to obtain the time-domain response.

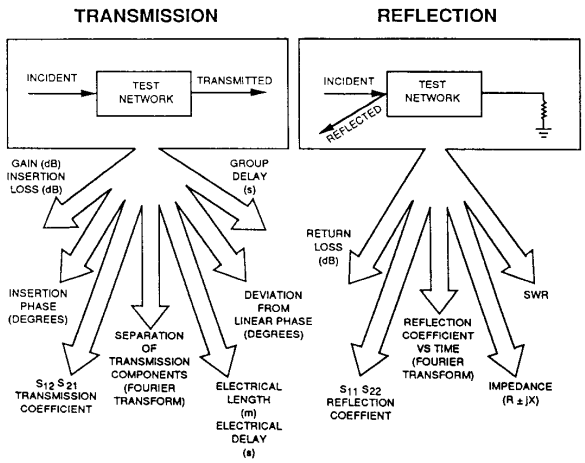

Fig. 5. Transmission and reflection measurements (after *HP 8510 Network Analyzer Operating and Programming Manual*, Hewlett-Packard Company, Santa Rosa, CA, 1984).

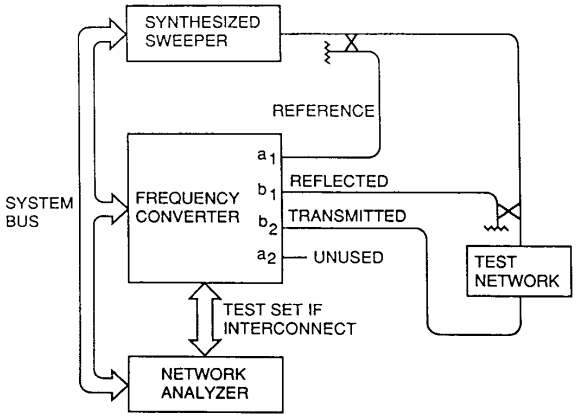

Fig. 6. Configuration of a network analyzer for transmission and reflection measurements.

As an example, Figure 6 illustrates the basic components of an HP 8510 vector network analyzer system, used for making transmission-reflection measurements. In general, the principles are the same for other vector network analyzer systems. The Hewlett Packard equipment will be stressed throughout this paper because the authors are more familiar with its operation. The system of Figure 6 consists of three pieces of equipment: (1) an HP 8340A or HP 8341A synthesized sweeper, which serves as the RF source; (2) an HP 8511A frequency converter, which serves as the RF-to-IF converter; and (3) an HP 8510A network anal-

yzer and display-processor, which serves as the IF detector, A/D converter, and digital processor.

The HP 8511A has four ports to which signals can be applied. Of these ports, the a_1 and a_2 ports are used to input the reference signal, and the b_1 and b_2 ports are used to input the measurement signals. In the basic transmission-reflection configuration (see Figure 6), a sample of the signal from the RF source is applied to the a_1 reference port, while the a_2 port is unused. The transmitted and reflected signals are then applied to the b_1 and b_2 measurement ports, respectively. The network analyzer can now give the magnitude and phase of the reflected and transmitted signals relative to that of the incident signal by forming the ratios

$$S_{11} = \frac{b_1}{a_1} \quad \text{and} \quad S_{21} = \frac{b_2}{a_1}, \tag{35}$$

respectively. Other characteristics of the network, as shown in Figure 5, can also be determined.

4.1 Network Analyzer Operation as a Scatterometer

The measurement system of Figure 6 can be reconfigured to allow operation as a scatterometer. In the scatterometer configuration, the "test network" is simply some radar target separated from the measurement system by free space. In this case, the signal from the RF source is coupled to free space with an antenna, and travels to the target (i.e., test network) through the air medium, instead of through a coaxial cable or waveguide. The signal reflected from the target is then received with another antenna, and is compared with a sample of the transmitted signal from the RF source, as before. The system can be configured as either a dual-antenna system or a single-antenna system (using a circulator to separate the transmitting and receiving channels) as shown in Figure 7.

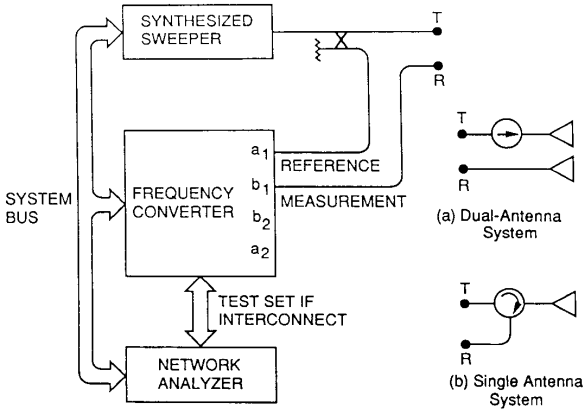

Fig. 7. Configuration of a network analyzer for scatterometer measurements: (a) dual-polarized single-antenna system, (b) single-antenna system.

There is a major difference between the transmission-reflection configuration and the scatterometer configuration. When operating as a scatterometer, there is a relatively long time delay between the returned and transmitted signals, due to propagation to the target and back. During this delay, the reference signal has changed frequency by an amount Δf, which corresponds to a phase error in degrees of $\Delta\phi = 360\Delta f\tau$, where $\tau = 2r/c$ is the two-way time delay. If a synthesized source is used, the transmitted signal can be stepped in frequency instead of continuously swept, to keep the reference signal at the same frequency as the received signal. However, any phase instability in the source can also produce a phase error. To operate as a coherent system, this phase error must be smaller than a few degrees over the delay time, τ. The phase stability over typical scatterometer ranges ($r \leq 20$ m, or $\tau \leq 133$ ns) for synthesized sweepers is negligible, so the phase error can be ignored. For a scatterometer with a continuously swept frequency, the phase error in degrees is related to τ and the sweep rate, f_s (in Hz s^{-1}) by the relationship $\Delta\phi = 360\, f_s\tau^2$, where $\Delta f = f_s\tau$. For the phase error to be less than one degree, the two-way phase delay, τ, must satisfy

$$\tau \leq \sqrt{\frac{1}{360 f_s}}\ . \tag{36}$$

A typical sweep rate for the HP 8510 system is f_s=20 MHz ms^{-1}, requiring $\tau \leq 373$ ns (or $r \leq 56$ m). This range is at least twice as large as typical scatterometer ranges, so network analyzers can usually operate effectively as scatterometers by using either synthesized (stepped) frequency or swept-frequency sources.

We have so far considered only a single polarization for transmitting and receiving; therefore, the system in Figure 7 represents a traditional (magnitude-only) scatterometer. It must be modified to operate as a polarimetric scatterometer. A polarimetric scatterometer, using the fully coherent approach, must be able to transmit and receive a set of orthogonal polarizations. The v and h linear polarizations will be used here for illustrative purposes. For the single-antenna system, we can add a second polarization channel and apply it to the b_2 port of the HP 8511A. For the dual-antenna system, two options are available. An additional channel can be utilized, similar to the single-antenna system, or polarizers can be inserted before the antennas. These different configurations are shown in Figure 8, where the network analyzer is assumed to be configured the same as in Figure 7.

There are several features available with most network analyzers which are particularly useful in scatterometer applications. One of these features is the ease with which the network analyzer can be programmed and controlled by a computer over an interface bus. This feature is stressed because it reduces the hardware design to the consideration of only RF components, as in Figure 8. The network analyzer supplies all the detection, processing, and data transfer options.

One of the most useful processing options available with many network analyzers is time-domain operation. Because the returned signal is measured as a function of frequency, real-time Fourier transform techniques can be used to obtain the time-domain response. In scatterometer applications, the result is a measure of the radar return as a function of range. In addition, all other processing operations are

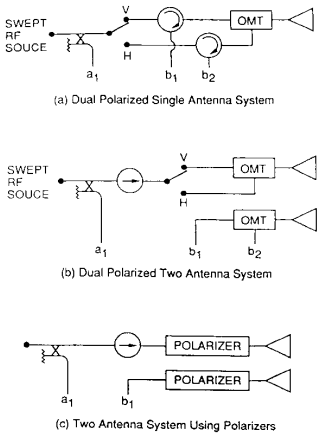

Fig. 8. Polarimetric configurations of a network- analyzer-based scatterometer: (a) dual-polarized single-antenna system, (b) dual-polarized-antenna system, and (c) dual-antenna system using polarizers.

available to both the time and frequency domains. Suppose a measurement of the backscattered power is desired, as a function of depth, for a volume of scatterers. By using the time-domain option with time-gating, the portion of the returned signal corresponding to a particular depth in the volume can be selected. The position and width of the time gate determines the range and range extent of the small volume within the entire volume of scatterers. The time-gated signal can then be transformed back to the frequency domain, to obtain the frequency response of the small volume, as modified by the medium between it and the scatterometer. This process is illustrated in Figure 9.

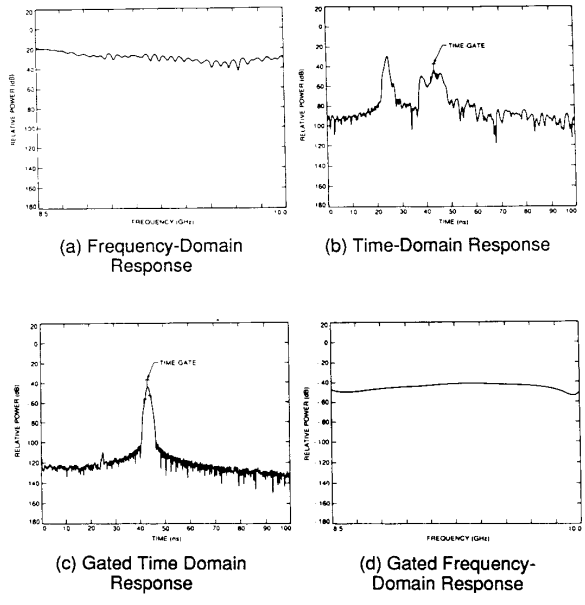

Fig. 9. Plots illustrating the use of gating with the time-domain option to measure the frequency response as a function of depth within a random medium: (a) frequency domain response, (b) time domain response, (c) gated time-domain response, and (d) gated frequency-domain response.

The range-resolution capability of the system is determined by the swept-frequency bandwidth, B,

$$\Delta r = \frac{c}{2B} \tag{37}$$

where c is the velocity of light. For the example shown in Figure 9, B = 1.5 GHz, and the corresponding range resolution is 10 cm. In the case of polarimetric scatterometers used for field operation, the bandwidth usually is selected to be on the order of 10–20% of the center frequency in the microwave band, and on the order of 2 GHz in the millimeter-wave band.

The network-analyzer system can also be used to remove spurious responses in the return signal. For example, scattering from objects other than the target can contribute to the noise of the measurement. Many network analyzers have data storage and complex math features which can remove these spurious responses. First, the response of the test setup without the target is stored, and later subtracted from the response when the target is present, resulting in a measurement of the target response, alone. The leakage signals caused by multiple reflections within the RF circuitry, that appear at the target range, can be removed in the same manner. An example illustrating this procedure is given in Figure 10.

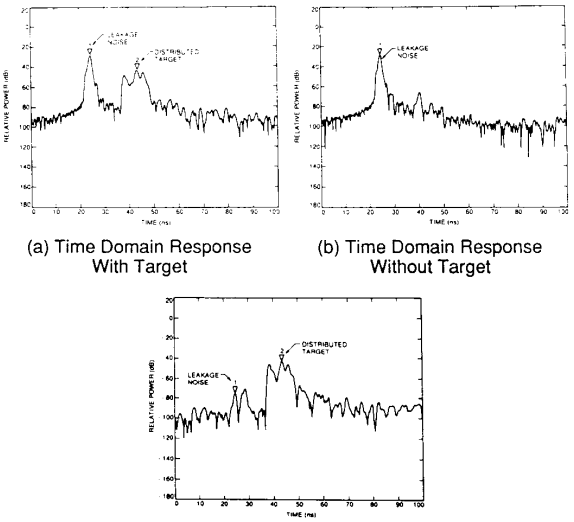

Fig. 10. Plots illustrating the use of complex mathematical operations with trace storage to remove leakage signals: (a) time-domain response with target, (b) time-domain response without target, and (c) time-domain response after subtraction of (b) from (a).

5. Polarimetric Scatterometers

5.1 Microwave Polarimetric Scatterometers

Scatterometers must be able to measure targets with a wide range of radar cross sections. In practice, targets with large radar cross sections are easy to measure, but there is a lower bound on the measurable RCS. This lower bound (minimum detectable target) for a given scatterometer at a fixed range from the target is limited by three major factors. The first factor is the thermal noise level, which is the abso-

lute minimum detectable level, and is determined by the receiver noise figure and system bandwidth. The second limiting factor is the dynamic range of the network analyzer's sampler (or mixer). This problem arises when a single antenna is used, or if there is insufficient isolation between the transmitting and receiving antennas. In such cases, part of the transmitted signal returns to the receiver's sampler and sets the minimum-detectable signal level. This minimum signal level can be determined by dividing the returned signal level by the dynamic range of the sampler. Finally, the third limiting factor is the effect of multiple reflections that appear at the target range. In a radar system, there usually exists an impedance mismatch between different RF components, and between the antenna and free space. A fraction of the transmitted signal, corresponding to each mismatch interface, returns to the receiver as noise. Multiple reflections between the mismatch interfaces also arrive at the receiver, but with different time delays corresponding to the total path length. The short-range reflections can be distinguished from the target signal in the time domain, but multiple reflections that appear at the target range cannot be separated from the target signal. Therefore, targets with a signal level that is less than the level of the multiple reflections are not detectable.

Because a network analyzer is a coherent device, its bandwidth is very narrow, and thermal noise is usually not a limiting factor. However, the dynamic range and multiple reflection problems limit the performance of scatterometers, but their adverse effects can be overcome by improving the isolation between the transmitting and receiving channels of the system.

The two basic schemes for configuring the antenna systems of typical scatterometers were shown in Figure 7. The single-antenna system, shown in Figure 7(a), isolates the transmitting and receiving channels by using a circulator. The isolation is typically on the order of 20 dB, and it is limited by leakage through the circulator, and by reflection from the mismatch at the antenna. Better isolation is obtained by using the dual-antenna system, shown in Figure 7(b). With this configuration, the isolation is limited by the coupling between the antennas, and it is on the order of 50 dB. Although the isolation is superior, there are other physical limitations for the dual-antenna system at microwave frequencies that make a single-antenna system more practical.

To study the characteristics of distributed targets as a function of incidence angle, a scatterometer must have a small angular resolution. This condition is usually achieved by using a small-beamwidth antenna. However, a decrease in beamwidth requires an increase in the size of the antenna aperture. At microwave frequencies, the aperture size becomes too large for dual-antenna systems to be practical. Aside from the obvious increase in weight, the increase in aperture size causes parallax problems, due to the large boresight separation between the transmitting and receiving antennas. In this case, the radar is no longer operating in the backscatter mode, and the antenna boresight directions must be adjusted, depending on the target range.

As mentioned, one of the disadvantages of single-antenna systems is the problem associated with the dynamic range limitations of network analyzers. For small targets, or for those that are far from the scatterometer, we may need to add amplifiers in the transmitting or receiving channels. However, the strong short-range signal returns, from the antenna mismatch and leakage from the circulator, may saturate

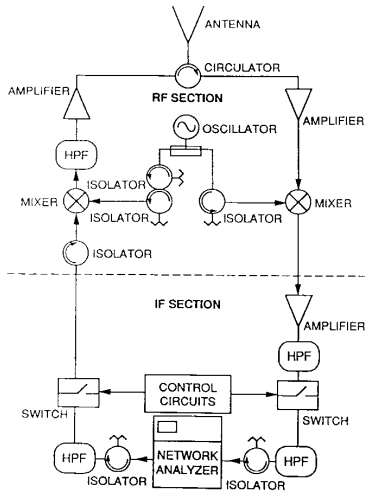

Fig. 11. Diagram of scatterometer system with switching.

the receiver. To reduce the level of these direct returns, a pulsing technique may be used [12, 13]. In this scheme, the receiver is switched off between transmission and when the signal return from the target arrives at the receiver. Because this switching is done at a much higher rate than the bandwidth of the receiver, the network analyzer does not sense that the incoming signal is pulsed, and it is measured as if it were a CW signal. The pulsing switches are placed in the transmitting and receiving channels as in Figure 11. The isolators and high-pass filters are used to remove switching transients which affect the response of the network analyzer. Note that the pulsing network is not interfaced with the network analyzer, and the pulsing operation is independent of the

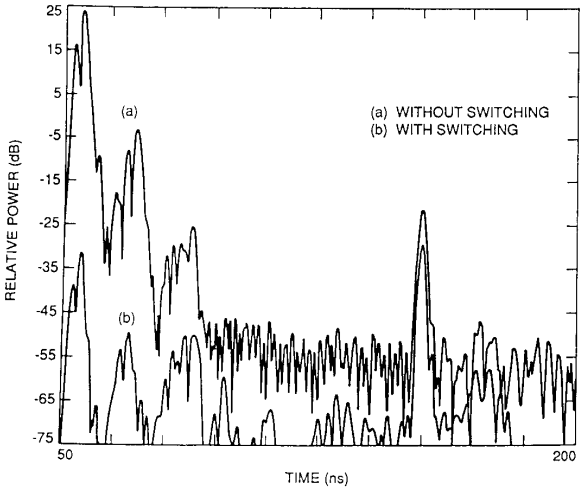

Fig. 12. Time-domain response of the system in an anechoic chamber: (a) without switching, (b) with switching.

network analyzer operating sequence. Figures 12 and 13 show two time- and frequency-domain responses of a target, with and without switching. When pulsing is applied, the short-range returns, which were dominant without pulsing, decrease significantly, and the target return decreases only slightly, by an amount dependent on the duty cycle. The overall signal-to-noise improvement in this example is about 10 dB.

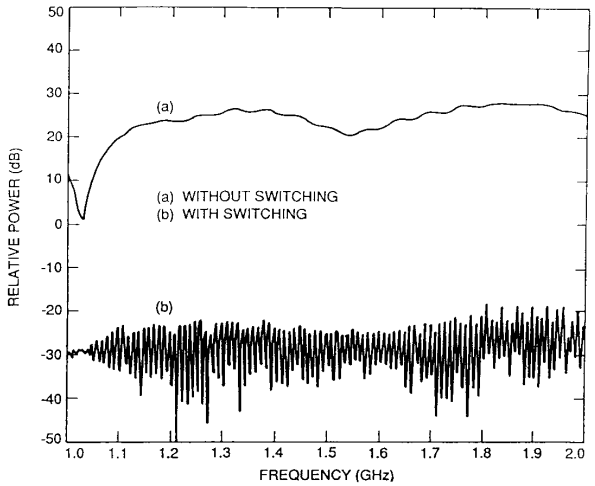

Fig. 13. Corresponding frequency-domain trace: (a) without switching, (b) with switching.

Figure 14 shows a photograph of the University of Michigan's truck-mounted microwave polarimetric scatterometer. The system operates at center frequencies of 1.25, 5.3, and 9.75 GHz, with each frequency channel having its own antenna and RF circuitry, but with all three sharing the same network analyzer. A similar system is also available for operation at millimeter wavelengths (35, 94, 140, and 215 GHz). These systems are used to study the scattering properties of trees, rough surfaces, snow-covered terrain, and other types of distributed targets.

Fig. 14. Photograph of the antenna and RF sections of POLARSCAT, which operates at 1.25, 5.3, and 9.75 GHz.

5.2 Millimeter-Wave Polarimetric Scatterometers

The free-space loss associated with the propagation of electromagnetic waves is inversely proportional to the square of the wavelength. If the wavelength is reduced by a factor of 10 (100 GHz instead of 10 GHz), the free-space loss increases by 20 dB. For a millimeter-wave polarimetric scatterometer, with the same beamwidth and performance as a microwave system, we must either increase the transmitted power or reduce the absolute noise level of the system. Because higher power is more difficult to obtain at millimeter-wave frequencies, the most reasonable option is to reduce the noise level. In the microwave system, a single antenna was used because of antenna size limitations, and we found that reflections from the antenna mismatch caused significant noise problems. These noise problems were somewhat improved by adding a pulsing network to remove the major contribution. Much of the noise associated with the single-antenna system can be avoided by using two antennas, which is the usual approach adopted with short-range millimeter-wave systems. Because millimeter-wave antennas (with beamwidths comparable to those in the microwave region) are much smaller, dual-antenna systems are not limited by the size of the antennas.

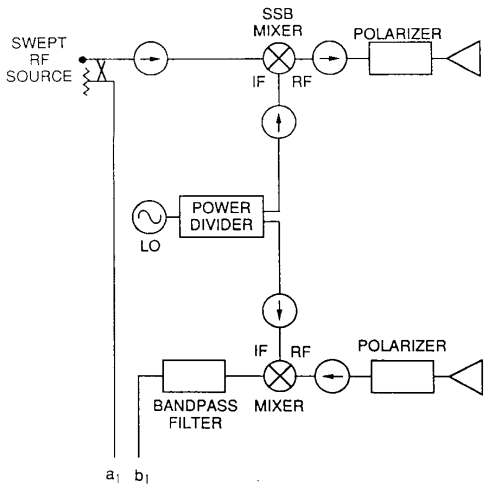

Fig. 15. Basic millimeter-wave polarimetric scatterometer.

The diagram in Figure 15 illustrates a basic polarimetric scatterometer design for millimeter-wave frequencies. To obtain a swept millimeter-wave frequency for transmission, a lower IF (typically in the 1–5 GHz range) is up-converted to the desired RF band, by using a single-sideband (SSB) up-converter, which passes only the frequency $f_{RF} = f_{LO} + f_{IF}$. The down-conversion stage used on reception passes only the difference frequency, $f_{IF} = f_{RF} - f_{LO}$. Because the up-conversion and down-conversion stages are driven by the same LO (local oscillator), phase coherence is maintained. To reduce the LO power requirements, we can use only one transmitting and one receiving channel (i.e., using only two mixers), and this can be accomplished by using polarizers to provide the polarization agility. The two isolators located at the LO ports of the mixers help to isolate the transmitting and receiving channels, by rejecting any leakage components traveling through the LO path. Isolators may be needed throughout the system, to reduce the multiple reflections discussed in Section 4.

At millimeter-wave frequencies (above about 120 GHz), the available LO power becomes so low that a single LO may not be able to drive both the up-conversion and down-conversion mixers. However, available LO power can be increased by injection phase-locking two separate sources. Figure 16 illustrates one way in which this can be done. All three sources of Figure 16 are designed to operate at the desired LO frequency. The oscillator-circulator combination acts as an unstable amplifier, the output power of which is approximately equal to that of the oscillator. The result is two coherent LO outputs, each with the power of a single oscillator.

6. Coherent-on-Receive Polarimetric Scatterometer

Consider a two-antenna system equipped with polarizers which can selectively switch either antenna to

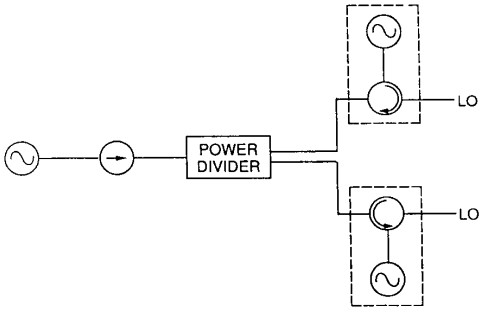

Fig. 16. Design used to phase-lock two LO sources.

v or h polarization. To measure all four elements of the scattering matrix, S, of a given point or distributed target, it is necessary to conduct a sequence of four separate measurements, corresponding to the four different combinations of transmit and receive polarizations. To take advantage of the range-gating capability of the network-analyzer system, it is necessary to operate in a stepped-frequency mode, which involves stepping the RF frequency in discrete increments over the desired bandwidth. In this mode, it takes on the order of 1 s to complete the desired sequence of measurements. Measurement time can be reduced down to 1 ms using a fast CW mode, but at the expense of range information.

With careful design, it is possible to maintain phase coherence in the system over the 1-s time interval when operating in the stepped-frequency mode. Under field conditions, however, slight fluctuations of the antenna platform or random movements of vegetation elements can cause significant phase variations at millimeter wavelengths. This problem is circumvented by the coherent-on-receive configuration, shown in Figure 17, which was proposed by Walter Flood [14], and implemented by both the University of Michigan and The University of Massachusetts [15]. The transmit antenna structure includes two parallel quarter-wave polarization phase plates, each of which is independently rotatable in its own plane. This feature allows the generation of any polarization configuration of interest, including vertical (v), horizontal (h), 45° linear (45), and left-hand circular (L), which are used, as discussed below, to obtain the 16 elements of the Mueller matrix. The receive antenna includes a 45° polarization grid, which allows separation of the v

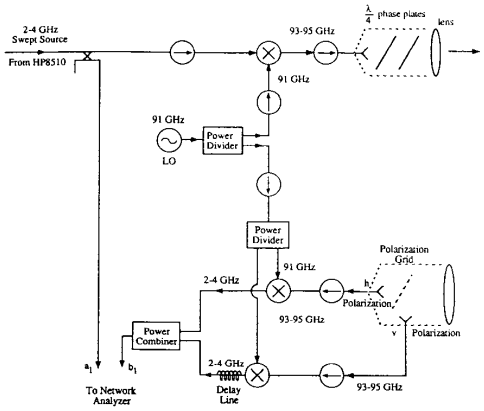

Fig. 17. Block diagram of a coherent-on-receive scatterometer.

and h components of the received signal. After down converting the two receive channels to IF, the signal in the v channel is delayed by a 20-m long delay line, and then the two signals are combined and sent to the network analyzer. The presence of the delay line serves to artificially shift the range location of the v-polarized signal (Figure 17), thereby allowing the measurement of both polarization components of the received signal, E_v^r and E_h^r, simultaneously. This is the reason for calling this technique a coherent-on-receive scatterometer.

To show how this technique can provide polarimetric scattering data, let us return to (28) and rewrite it in the following form:

$$\mathbf{F}_m^r = \begin{bmatrix} F_1^r \\ F_2^r \\ F_3^r \\ F_4^r \end{bmatrix} = \frac{1}{r^2} \begin{bmatrix} L_{11} & L_{12} & L_{13} & L_{14} \\ L_{21} & L_{22} & L_{23} & L_{24} \\ L_{31} & L_{32} & L_{33} & L_{34} \\ L_{41} & L_{42} & L_{43} & L_{44} \end{bmatrix} \begin{bmatrix} F_1^t \\ F_2^t \\ F_3^t \\ F_4^t \end{bmatrix} \tag{38}$$

where F_1^r to F_4^r are the four Stokes parameters of the received Stokes vector, all of which are determined directly from the measured fields, E_v^r and E_h^r. The 16 elements, L_{11} to L_{44}, are the components of the Mueller matrix $\mathscr{L}_m$, and F_1^t to F_4^t are the Stokes parameters of the transmitted Stokes vector.

Our objective is to measure the elements of $\mathscr{L}_m$. This can be achieved by measuring $\mathbf{F}^r$ for each of four different incident polarizations, namely, vertical, horizontal, 45° linear, and left circular, whose Stokes vectors are given by

$$\mathbf{F}_v^t = \begin{bmatrix} 1 \\ 0 \\ 0 \\ 0 \end{bmatrix} I_0,\ \mathbf{F}_h^t = \begin{bmatrix} 0 \\ 1 \\ 0 \\ 0 \end{bmatrix} I_0,\ \mathbf{F}_{45}^t = \begin{bmatrix} 1/2 \\ 1/2 \\ 1 \\ 0 \end{bmatrix} I_0,\ \mathbf{F}_L^t = \begin{bmatrix} 1/2 \\ 1/2 \\ 0 \\ 1 \end{bmatrix} I_0. \tag{39}$$

The received Stokes vectors, measured in response to $\mathbf{F}_v^t$ and $\mathbf{F}_h^t$, lead to a determination of the elements in the first and second columns of $\mathscr{L}_m$, respectively. The third and fourth columns can be obtained from the received Stokes vectors corresponding to the following two linear combinations of transmit Stokes vectors:

$$\mathbf{F}_a^t = \mathbf{F}_{45}^t - \frac{1}{2}\left[\mathbf{F}_v^t + \mathbf{F}_h^t\right] = \begin{bmatrix} 0 \\ 0 \\ 1 \\ 0 \end{bmatrix}$$

$$\mathbf{F}_b^t = \mathbf{F}_L^t - \frac{1}{2}\left[\mathbf{F}_v^t + \mathbf{F}_h^t\right] = \begin{bmatrix} 0 \\ 0 \\ 0 \\ 1 \end{bmatrix}. \tag{40}$$

This process of measuring $\mathscr{L}_m$ can be repeated for as

many independent samples as desired. To reduce the uncertainty, associated with signal fading variations, such that the 90% confidence interval is about ± 0.6 dB, N must be on the order of 50 [16, p. 49]. With $\langle \mathcal{L}_m \rangle$ known, we can use (31) and (33) to compute σ^o for any combination of transmit and receive antenna polarizations.

7. Calibration

The calibration problem can be modeled in terms of the generalized schematic representation shown in Figure 18, which represents the condition when the polarization switch of the transmitting antenna is set to transmit a vertically-polarized wave of amplitude E_0. For an ideal, distortion-free antenna, the transmitted field, $\mathbf{E}^t$, consists of only a vertically-polarized component, E_0, and no horizontally-polarized energy is emitted. In reality, however, the transmitted field consists of a vertically-polarized component, $T_{vv}E_0$, and a horizontally-polarized component, $T_{hv}E_0$, where T_{hv} represents the coupling between the v- and h-channels of the antenna. A similar situation occurs for the receive antenna, as shown in Figure 18. This departure from the ideal is called polarization distortion, and is usually characterized in terms of distortion matrices.

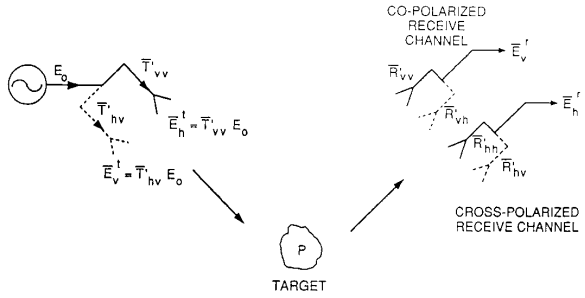

Fig. 18. Schematic representation of transmitting and receiving antennas for v-polarized transmitting configuration. The dashed lines represent polarization coupling. For an antenna with perfect polarization isolation, the coupling coefficients would be zero.

For the situation shown in Figure 18, the measured received electric field is given by

$$\mathbf{E}^r = \begin{bmatrix} E_v^r \\ E_h^r \end{bmatrix} = e^{i\phi}\frac{K}{r^2}\begin{bmatrix} R_{vv} & R_{vh} \\ R_{hv} & R_{hh} \end{bmatrix}\begin{bmatrix} S_{vv} & S_{vh} \\ S_{hv} & S_{hh} \end{bmatrix}\begin{bmatrix} T_{vv} \\ T_{hv} \end{bmatrix} \tag{41}$$

where

$$K = \left[\frac{2\eta_0 P_t G_t G_r \lambda^2}{(4\pi)^2}\right]^{1/2} . \tag{42}$$

The elements of the **S** matrix are the scattering parameters to be measured, the elements of the **R** matrix are the distortion components of the receive antenna distortion matrix, $P_t = E_0^2/2\eta_0$ is the transmitted power, G_t and G_r are the nominal gains of the transmit and receive antennas, $\phi = 2k_0 r$ is a phase factor which accounts for two-way propagation between the target and the radar, and r is the range to the target. If the radar system uses distortion-free or approximately distortion-free antennas, with $R_{vv} \simeq R_{hh} \simeq T_{vv} \simeq 1$ and $R_{vh} \simeq R_{hv} \simeq T_{hv} \simeq 0$, the expression for $\mathbf{E}^r$ simplifies to

$$E_v^r = e^{i\phi}\frac{K}{r^2} S_{vv} ,$$

$$E_h^r = e^{i\phi}\frac{K}{r^2} S_{hv} . \tag{43}$$

A repeat of the process, with the transmit antenna illuminating the target with a horizontally-polarized wave, leads to expressions in terms of S_{hh} and S_{vh}. For polarization-synthesis applications, it is not necessary to know the absolute phases of the four scattering amplitudes; we need to know the phases of any three of them relative to the fourth. Hence, the factor $e^{i\phi}$, being common to all four, need not be determined. Finally, the constant, K, can be determined by performing a calibration measurement against a target with known scattering matrix, such as a metal sphere or a metal cylinder.

For the general case, where the antennas are not close to being distortion free, the calibration problem calls for a more complicated procedure, often involving measurements of more than one calibration target. The interested reader is referred to [11, 17-20].

8. Personal Concluding Remarks by F.T. Ulaby

When I designed and built my first FM scatterometer in 1970, it took me three months to connect all the equipment together, and another three months to get the system to work properly. It was many months later before my graduate students and I had the system calibrated, and its performance evaluated. All operations were manually controlled from a front panel covered with switches and knobs.

My fourth-generation scatterometer was built in 1981. It was computer-controlled, and much more compact and reliable than its predecessors. However, it took over a year to "computerize" the system, which included the construction of circuit cards to interface the computer to the various subsystems, writing the control software, and forever debugging it!

In today's world, a student familiar with the operation of the Automatic Vector Network Analyzer (which our students learn to use in their microwave laboratory courses) can put together a basic scatterometer and evaluate its performance in a matter of hours! There is still a great deal of work that needs to be done to design and build a high-performance scatterometer; however, the effort is spent in optimizing the performance of the antenna and RF circuits, rather than in designing and building the low-frequency signal-processing and control circuitry.

References

[1] Ulaby, F.T. and C. Elachi, *Radar Polarimetry for Geoscience Applications*, Norwood, Massachusetts, Artech House, 1990.

[2] *IEEE Standard Test Procedures for Antennas*, New York, IEEE Press, 1979.

[3] Sinclair, G., "The Transmission and Reception of Elliptically Polarized Waves," *Proc. IRE*, **38**, 148-151, 1950.

[4] Kennaugh, E.M., "Effects of the Type of Polarization on Echo Characteristics," Report 389-9, Antenna Laboratory, Ohio State University, 1951.

[5] Van de Hulst, H.C., *Light Scattering by Small Particles*, New York, Dover, 1981, pp. 28-42.

[6] van Zyl, J.J., "Unsupervised Classification of Scattering Behavior Using Imaging Radar Polarimetry Data," *IEEE Trans. Geosci. Remote Sensing*, **GE-27**, 36-45, 1989.

[7] van Zyl, J.J., H.A. Zebker, and C. Elachi, "Imaging Radar Polarization Signatures: Theory and Observation," *Radio Science*, **22**, 529-543, 1987.

[8] Ulaby, F.T., T.F. Haddock, J. East, and M.W. Whitt, "A Millimeter-Wave Network Analyzer Based Scatterometer," *IEEE Trans. Geosci. Remote Sensing*, **GE-26**, 75-81, January 1988.

[9] Whitt, M.W., and F.T. Ulaby, "Millimeter-Wave Polarimetric Measurements of Artificial and Natural Targets," *IEEE Trans. on Geosci. Remote Sensing*, **GE-26**, 562-573, September 1988.

[10] Blanchard, A.J., and J. Rochier, "Bistatic Radar Cross Section Measurement Facility," *Proceeding of IGARSS '87 Symposium*, Ann Arbor, MI, Vol. I, pp. 545-548, May 1987.

[11] Riegger, S., W. Wiesbeck, and A.J. Sieber, "On the Origin of Cross-Polarization in Remote Sensing," *Proceedings of IGARSS '89 Symposium*, Ann Arbor, MI, Vol. 1, pp. 577-580, May 1987.

[12] Tassoudji, M.A., K. Sarabandi, and F.T. Ulaby, "Design Consideration and Implementation of the LCX Polarimetric Scatterometer (POLARSCAT)," Rep. No. 022486-T-2, Radiation laboratory, The University of Michigan, Ann Arbor, June 1989.

[13] Liepa, V.V., K. Sarabandi, and M.A. Tassoudji, "A Pulsed Network Analyzer Based Scatterometer," *Proceedings of IGARSS '89 Symposium*, Vancouver, British Columbia, pp. 1826-1828, July 10-14, 1989.

[14] Flood, W., Army Research Office, Personal Communication.

[15] Mead, James B., "Polarimetric Measurements of Foliage and Terrain at 225 GHz", PhD Thesis, University of Massachusetts, February, 1990.

[16] Ulaby, F.T. and M.C. Dobson, *Handbook of Radar Scattering Statistics for Terrain*, Artech House, Norwood, Massachusetts, 1989.

[17] Sarabandi, K., F.T. Ulaby, and M.A. Tassoudji, "Calibration of Polarimetric Radar Systems with Good Polarization Isolation," *IEEE Trans. on Geosci. Remote Sensing*, **GE-28**, 1990.

[18] Barnes, R.M., "Polarimetric Calibration Using Inscene Reflectors," Rep. TT-65, MIT Lincoln Laboratory, Lexington, MA, September 1986.

[19] van Zyl, J.J., "Calibration of Polarimetric Images Using Only Image Parameters and Trihedral Corner Reflector Responses," *IEEE Trans. Geosci. Remote Sensing*, **GE-28**, 1990.

[20], M.W., F.T. Ulaby, P. Polatin, and V. Liepa, "A General Polarimetric Calibration Technique," *IEEE Trans. Ant. Prop.*, **AP-38**, 1990.

CORRECTION

The article, which began on page 50 of the February, 1990, issue of the *Magazine*, was authored by John Cavanaugh. The *Magazine* apologizes for the omission of his name from this report on the CCIR Study Group 5 final meeting.

INTRODUCING FEATURE ARTICLE AUTHOR

Francis X. Canning

Francis X. Canning was born in Summit, New Jersey, in September, 1950. After a freshman year at SUNY at Stony Brook, he transferred to Dartmouth College. Unable to decide on a major, he completed both the mathematics and physics majors, receiving the AB degree in March of 1971. This dual interest continued on into graduate school, at the University of Massachusetts at Amherst. Ultimately concentrating on physics, he studied the statistical mechanics of solitons and of phase transitions, receiving the MS degree in 1976 and the PhD in 1982. He then worked on electromagnetic wave propagation and scattering at the Naval Weapons Center at China Lake from 1982 to 1987, first using high-frequency methods, and later becoming interested in developing more efficient "numerical" methods. This work is continuing at the Rockwell Science Center, where he now uses an eclectic approach in his research, as exemplified by this article.